

Investigation of the threshold anomaly for the ${}^7\text{Li} + {}^{159}\text{Tb}$ systemD. Patel,^{1,2,3,*} S. Mukherjee,^{1,†} D. C. Biswas,³ B. K. Nayak,³ Y. K. Gupta,³ L. S. Danu,³ S. Santra,³ and E. T. Mirgule³¹*Physics Department, Faculty of Science, M. S. University of Baroda, Vadodra-390002, India*²*Department of Applied Physics, Sardar Vallabhbhai National Institute of Technology, Surat-395007, India*³*Nuclear Physics Division, Bhabha Atomic Research Centre, Mumbai-400085, India*

(Received 30 July 2014; revised manuscript received 16 April 2015; published 18 May 2015)

Elastic-scattering angular distributions were measured for the ${}^7\text{Li} + {}^{159}\text{Tb}$ system at various energies; namely, 24, 26, 28, 30, 35, 40, and 44 MeV. The optical-model analysis was performed to investigate the energy dependence of real and imaginary potentials, employing a Woods–Saxon form of potential. The dispersion-relation analysis were also carried out to check the consistency of real and imaginary parts of the potentials. The energy dependence of real and imaginary potentials does not follow the trend of conventional threshold anomaly but rather represents unusual behavior of the increase of imaginary part of the potential and corresponding decrease in real part of the potential near the Coulomb barrier energy. The effect of breakup coupling on elastic-scattering angular distributions was studied by a continuum-discretized coupled-channels (CDCC) calculation. The behavior of dynamic polarization potentials obtained due to the breakup coupling is discussed. The total reaction cross sections for the present and various other systems are also compared involving ${}^7\text{Li}$ projectile on different target nuclei in the mass range $A = 16$ to 232.

DOI: [10.1103/PhysRevC.91.054614](https://doi.org/10.1103/PhysRevC.91.054614)

PACS number(s): 25.70.Bc, 25.70.Mn

I. INTRODUCTION

The study of interaction of loosely bound nuclei at near barrier energies has achieved considerable interest due to the availability of radioactive nuclear beam in the past few years [1,2]. In particular many efforts have been devoted to search for the fingerprints of the expected influence of their weak binding properties on the various reaction channels that occurs at near barrier energies, such as inelastic scattering, transfer, breakup, and fusion. The study of any particular behavior of the optical potential that describes the elastic scattering under the influence of these absorption channels is a key doorway. The most important features of the elastic scattering between heavy ions at energies close to the Coulomb barrier is the peculiar behavior of the optical potential, known as the “threshold anomaly” (TA) [3]. In brief, at higher energies the real and imaginary parts of the optical potential remain energy independent; however, as the energy is lowered toward the Coulomb barrier, the imaginary part of the optical potential sharply decreases while the real part presents a localized peak. The “TA” may be ascribed mainly to the coupling of the elastic scattering to other reaction channels that produces an attractive polarization potential ΔV , leading to the real potential $V = V_0 + \Delta V$, where V_0 is the real potential at higher energies. The behavior of the imaginary potential is associated with the closing of nonelastic peripheral channels at energies near and below the barrier. The TA is well established for the scattering of tightly bound nuclei. However, there are presently some speculative arguments and contradictory conclusions about the influence of the breakup (BU) of weakly bound nuclei which might affect the known behavior of TA. For systems in which at least one of the interacting participants is a weakly bound nucleus, the rapid decrease of the fusion cross

section does not imply the closing of all the reaction channels at the subbarrier energies. As a consequence of large peripheral-reaction cross section at these energies, the imaginary part of the optical potential does not necessarily decrease and the TA may disappear. Recently, it has been shown that the breakup (BU) channel does not diminish so fast in the vicinity of the Coulomb barrier; rather, it can have some magnitudes. It has been suggested that the effect of coupling of the BU channel to the continuum may produce a repulsive polarization potential that affects the overall dynamic polarization in such a way that the usual TA may vanish [1]. This fact has been taken as the possible explanation of the absence of usual TA for the systems involving the weakly bound nuclei ${}^6,{}^7\text{Li}$ or ${}^9\text{Be}$. There have been many measurements and theoretical studies for understanding the presence or absence of TA. In the case of tightly bound nuclei, the existence of TA is well understood that is due to the role of strong inelastic couplings. For example, in the elastic scattering of ${}^6,{}^7\text{Li}$ on ${}^{27}\text{Al}$ [4–6], ${}^{28}\text{Si}$ [7,8], ${}^{59}\text{Co}$ [9], ${}^{80}\text{Se}$ [10], ${}^{116}\text{Sn}$ [11,12], ${}^{138}\text{Ba}$ [13], ${}^{144}\text{Sm}$ [14], ${}^{208}\text{Pb}$ [15], and ${}^{232}\text{Th}$ [16] for ${}^7\text{Li}$ projectile, TA has been observed except for the target masses $A = 27, 28, 116,$ and 144 . On the contrary, for ${}^6\text{Li}$ projectile, some of the systems show the breakup threshold anomaly (BTA) with a possible explanation of its lower breakup threshold (~ 1.46 MeV) in comparison to ${}^7\text{Li}$ (~ 2.47 MeV). Because the breakup (BU) cross section does not decrease significantly in the vicinity of the Coulomb barrier, this is no longer the threshold of the closing of the reaction channels. The systematic results from the back scattering method has shown unique energy dependence for different targets but the same projectile, possibly due to the involvement of different reaction mechanisms, therefore different polarization potentials [17,18]. Considering the above discussion one may conclude that a systematic study for the behavior of optical-model (OM) potentials for such systems which involve weakly bound nuclei are required to have qualitative understanding of reactions with radioactive nuclei.

*dipika.physics@gmail.com

†smukherjee_msufpy@yahoo.co.in

The observation of TA or BTA certainly depends on breakup threshold energy of respective weakly bound nuclei and the presence of bound inelastic states, if any. These may produce the net polarization potential consisting of competing attractive and repulsive parts. The target structure also plays an important role, because it may produce a strong polarization potential, and the relative importance of the Coulomb breakup (BU) depends on the target mass.

The objective of the present work is to measure very precise and complete angular distribution at energies starting from below the Coulomb barrier to approximately twice this value, for the ${}^7\text{Li} + {}^{159}\text{Tb}$ system. The behavior of the optical potentials have been studied by optical-model analysis and the effect of breakup coupling is investigated by a continuum-discretized coupled-channels (CDCC) calculation. The dynamic polarization potentials (V_{pol} , W_{pol}), generated from breakup coupling have also been studied as a function of bombarding energy. In order to investigate the role of the breakup processes, the total reaction cross sections for the present system and several other systems are compared, which involve ${}^7\text{Li}$ projectile but different target nuclei in the mass range $A = 16$ to 232.

In Sec. II, the experimental details have been given. Section III presents an optical-model analysis and interpretation of the energy dependence of the optical potentials by using a Woods–Saxon form of the nuclear potential. Section IV describes the study of a coupled-channels calculation in terms of the CDCC formalism. The polarization potentials are also discussed in this section. Total reaction cross sections in the interaction of ${}^7\text{Li}$ projectile with different target nuclei are compared in the Sec. V. Finally, Sec. VI gives the summary of the present work and the main conclusions.

II. EXPERIMENTAL DETAILS

The experiment was performed at the BARC-TIFR Pelletron facility in Mumbai, India. The beam of ${}^7\text{Li}$ was delivered by the 14UD Pelletron accelerator covering the energy range from below to nearly twice the Coulomb barrier, i.e., 24, 26, 28, 30, 35, 40, and 44 MeV. The beam current during the entire experiment ranged from 20 to 40 nA. The beam was bombarded onto a self-supported enriched ${}^{159}\text{Tb}$ target of thickness 1 mg/cm^2 and the elastically scattered ${}^7\text{Li}$ ions were detected by four solid-state silicon surface barrier detector telescopes. The detector telescopes were of thickness (T_1) with $\Delta E = 25 \text{ } \mu\text{m}$ and $E = 300 \text{ } \mu\text{m}$ (T_2) with $\Delta E = 15 \text{ } \mu\text{m}$ and $E = 1.5 \text{ mm}$, (T_3) with $\Delta E = 15 \text{ } \mu\text{m}$ and $E = 1 \text{ mm}$ and (T_4) with $\Delta E = 15 \text{ } \mu\text{m}$ and $E = 1 \text{ mm}$. The telescopes were placed on a rotating arm inside a 1 m scattering chamber at an angular separation of 10° between consecutive telescopes, and M_1 and M_2 were placed at 15° and 20° , respectively. The measured statistical error in the data was less than 5% in the forward angles and less than 8% in the backward angles. Figure 1 shows a typical biparametric ΔE - E spectrum for the ${}^7\text{Li} + {}^{159}\text{Tb}$ system at $E_{\text{lab}} = 40 \text{ MeV}$ and $\theta = 40^\circ$. The inset of Fig. 1 shows the corresponding projection for the $Z = 3$ event. The measured elastic-scattering angular distributions normalized with Rutherford cross sections are shown in Fig. 2.

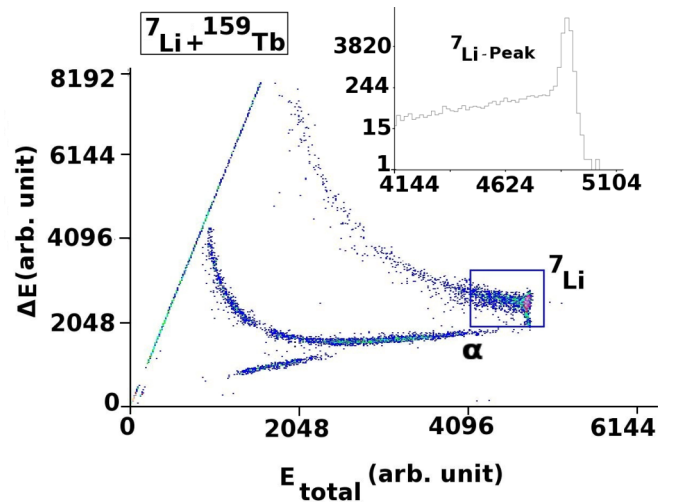


FIG. 1. (Color online) A typical biparametric ΔE - E spectrum for the ${}^7\text{Li} + {}^{159}\text{Tb}$ system at $E_{\text{lab}} = 40 \text{ MeV}$ and $\theta = 40^\circ$.

III. OPTICAL-MODEL ANALYSIS OF ELASTIC SCATTERING

The elastic-scattering angular distribution data are analyzed by using a phenomenological Woods–Saxon form of potential (WSP). The optical-model fits to the elastic-scattering data are performed using the ECIS code [19]. The WSP is an optical potential that has been successfully used to describe a large variety of systems in a wide range of energy, including fusion excitation functions and barrier distribution of weakly bound nuclei. In the fitting procedure, radius parameters were initially allowed to vary with fixed depths and diffuseness parameters for both the real and imaginary parts. In the next step, the diffuseness parameters were allowed to vary, but depths and radius parameters were fixed. The fitting procedure was repeated with constant radius $r = 7.7702 \text{ fm}$ [$r_0(A_p^{1/3} + A_t^{1/3})$, where $r_0 = 1.06 \text{ fm}$] and varying the diffuseness parameters from 0.66 to 0.74 fm in steps of 0.02 fm. A reasonably good fit to the data is obtained, but as usual several families of optical potential parameters are observed that describe the angular distributions equally well. To reduce the ambiguities with a different set of potentials, the radii of sensitivity R_{sr} and R_{si} , corresponding to the real and imaginary parts, are determined, where different curves of potentials have the same value [20,21]. The curves resulting from the present analysis using the WSP are shown in Fig. 2. Figure 3 shows different set of potentials that intersects at a common radii of sensitivity for 40 MeV laboratory energy. The average sensitive radius is $\sim 11.5 \text{ fm}$ (average between R_{sr} and R_{si} at different energies), along with the mean diffuseness $a_0 = 0.70 \text{ fm}$. The resulted fitting parameters from this analysis are listed in Table I.

In order to study the energy dependence of the real and imaginary potentials, the potential parameters are extracted at the radius of sensitivity ($\sim 11.5 \text{ fm}$) for the ${}^7\text{Li} + {}^{159}\text{Tb}$ system as shown in the Fig. 4. The related error bars in this figure represent the range of deviation of the potential corresponding to χ^2 variation of one unit. It can be observed that, as the energy decreases, the imaginary potential first increases and then

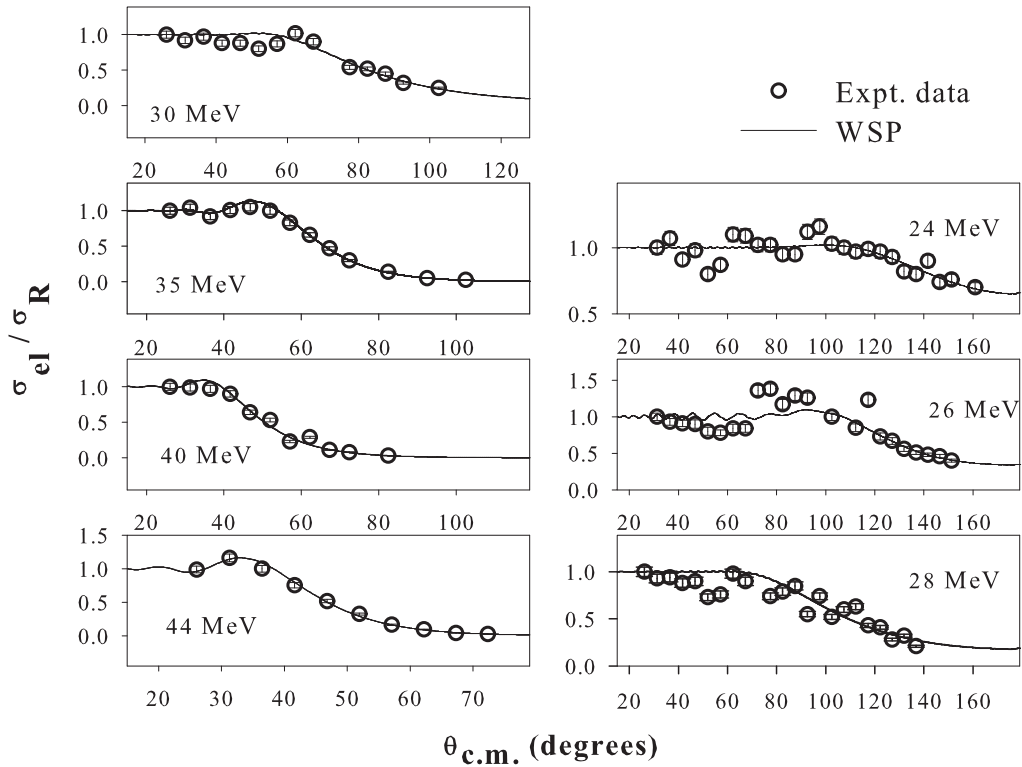


FIG. 2. Experimental elastic-scattering cross sections normalized to the Rutherford cross sections as a function of $\theta_{c.m.}$ and its best fit from optical-model analysis for the ${}^7\text{Li} + {}^{159}\text{Tb}$ system. The curves corresponding to best fit are obtained by using the Woods–Saxon potential (WSP).

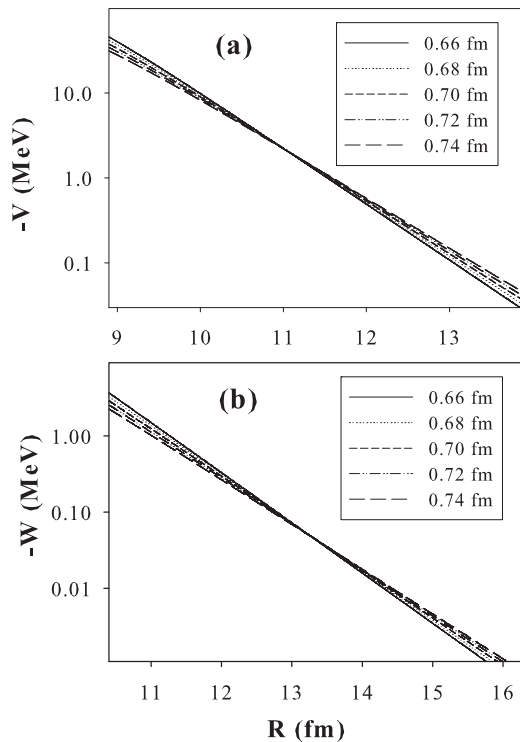


FIG. 3. Sensitivity radii based on the crossing of the (a) real and (b) imaginary parts of the WSP potential at $E_{\text{lab}} = 40$ MeV. The real and imaginary diffuseness, a_r and a_i , are varied in steps of 0.02 fm between 0.66 and 0.74 fm.

starts decreasing to zero, except for the lowest incident energy. The corresponding real potential more or less remains energy independent at near barrier energy. The present characteristics of real and imaginary potentials contradict the well-known behavior for the usual threshold anomaly which was observed for tightly bound systems. The dispersion-relation analysis also was carried out to check the consistency of behavior of the optical potentials as a function of energy. This study was done by using the expression that relates the real and imaginary parts of the potential [22]:

$$V(r; E) = \frac{P}{\pi} \int_0^{\infty} \frac{W(r; E')}{E' - E} dE'. \quad (1)$$

TABLE I. Optical-potential parameters and total reaction cross sections obtained from the optical-model (OM) analysis by using a Wood–Saxon form of potential (WSP) with $a_o = 0.70$ fm and $r = 7.7702$ fm [$r_0(A_p^{1/3} + A_t^{1/3})$, where $r_0 = 1.06$ fm] for the ${}^7\text{Li} + {}^{159}\text{Tb}$ system.

$E_{c.m.}$	V_o (MeV)	W_o (MeV)	χ_{min}^2/N	σ_R (mb)
22.99	187.09	19.11	2	50
24.90	139.37	1.61	4.7	106
26.82	8.68	168.7	4.92	532
28.73	13.97	386.4	2.27	1008
33.52	116.13	71.51	1.58	1150
38.31	124.98	226.76	3.4	1761
42.14	87.28	64.54	1.83	1614

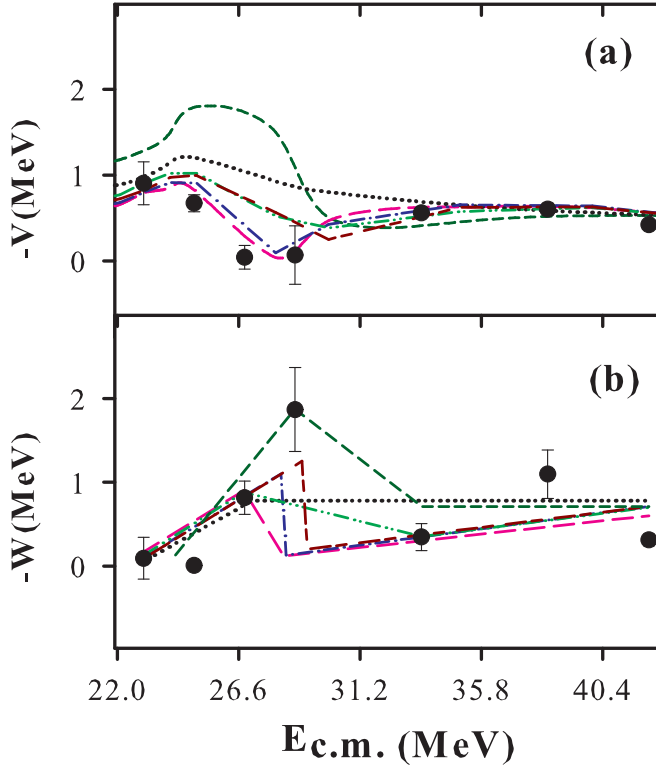


FIG. 4. (Color online) Energy dependence of the (a) real and (b) imaginary parts of the optical potential obtained for the ${}^7\text{Li} + {}^{159}\text{Tb}$ system at an average radius $R_s = 11.5$ fm. The energy V_b of the Coulomb barrier is ~ 26.6 MeV in the center-of-mass frame calculated using the Bass formula.

Also,

$$V(r; E) = V_o(r; E) + \Delta V(r; E), \quad (2)$$

where P is the principal value, and ΔV (polarization potential) and V_o are rapidly and smoothly varying functions with respect to energy. In this analysis two and three linear segments for imaginary potential are tried to calculate the corresponding real parts, as shown in Figs. 4(b) and 4(a), respectively.

It was observed that the calculated real potentials do not describe the experimental data points, when the energy dependence of imaginary potential is segmented into two linear parts as in the case of tightly bound systems. However, the consideration of the flat, increasing, and then decreasing trend of the imaginary potentials at above, near, and below barrier energy, respectively, can explain the nature of real potentials. This suggest that the conventional threshold anomaly cannot be confirmed from the present unusual observation for the energy dependence of real and imaginary potentials. Similar observations were reported in the past for the reaction of ${}^7\text{Li}$ projectile with ${}^{27}\text{Al}$ [4–6], ${}^{28}\text{Si}$ [7,8], ${}^{116}\text{Sn}$ [12], and ${}^{144}\text{Sm}$ [14] systems. The normal threshold anomaly, however, was reported for target masses such as ${}^{80}\text{Se}$ [10], ${}^{208}\text{Pb}$ [15], and ${}^{232}\text{Th}$ [16]. It may be concluded that, in the case of ${}^7\text{Li}$ projectile, the presence of the conventional threshold anomaly does not hold for all the target masses possibly due to the

occurrence of strong competition among breakup, transfer, and other nonelastic reaction channels.

IV. CONTINUUM-DISCRETIZED COUPLED-CHANNELS CALCULATIONS

With an aim to investigate the projectile breakup effect on elastic-scattering angular distributions, continuum-discretized coupled-channels calculation has been done by using the code FRESKO [29], version FRES 2.8. The method of coupled-channels calculations using the CDCC formalism has been widely studied in reactions which involve weakly bound nuclei [30–33]. The ${}^7\text{Li}$ (projectile) was considered as an $\alpha + t$ cluster and the continuum part was discretized in small momentum bins of finite width of $\Delta k = 0.20 \text{ fm}^{-1}$ for the nonresonant part and the resonant part was treated differently to avoid double counting. The bound excited state ($\frac{1}{2}^-$, 478 keV state) of ${}^7\text{Li}$ also was incorporated in the present calculation. The scattering wave functions in the solution of the coupled-channels calculations were integrated up to 140 fm in steps of 0.05 fm and the relative angular momentum was taken up to $110\hbar$. The maximum excitation energy was taken up to ~ 9 MeV. The cluster-folded potentials for the ${}^7\text{Li} + {}^{159}\text{Tb}$ were adjusted to obtain the optimum description of the elastic-scattering data and were fixed at 113.96 MeV with $r_o = 1.2$ fm, $a_o = 0.72$ fm and at 123.93 MeV with $r_o = 1.245$ fm, $a_o = 0.770$ fm for $t + {}^{159}\text{Tb}$ and $\alpha + {}^{159}\text{Tb}$, for all energy. The imaginary potentials were $W_o = 50.0$ MeV, $r_o = 1.06$ fm, and $a_o = 0.4$ fm. The binding potentials between the $\alpha + t$ cluster for bound and resonant states of ${}^7\text{Li}$ projectile that calculates the bin wave functions were taken from the Ref. [30]. In addition to the breakup channel, the target inelastic states were also included in the calculation. The transition strengths $[B(E2)]$ from (g.s., $\frac{3}{2}^+$) \rightarrow (0.058 MeV, $\frac{5}{2}^+$) and (0.1375 MeV, $\frac{7}{2}^+$) are $(2.8013 \pm 0.1458)e^2b^2$ and $(1.4736 \pm 0.2047)e^2b^2$, respectively, are taken from Ref. [34].

In the Fig. 5, the curves show the results of calculation with (solid line) and without (dashed line) breakup coupling. A reasonable description of the elastic-scattering data is obtained by the CDCC calculations. The breakup coupling effects are visibly small on the elastic-scattering cross section at energies above the barrier and it reduces as the barrier energy is approached. The polarization potentials also are obtained to investigate their behavior as a function of radius R , as shown in Fig. 6. It is observed that, as the projectile energy approaches the Coulomb barrier, the real part of the DPP (V_{dpp}) increases, showing the repulsive nature of the potential which is consistent with the observed behavior of the potential parameters from the OM analysis (Fig. 4). The corresponding imaginary part of the DPP (W_{dpp}) becomes more attractive as the energy decreases except the lowest incident energy. The real and imaginary parts of the dynamic polarization potentials (DPPs) that are obtained from the CDCC calculation, at a radius of sensitivity (~ 11.5 fm) for different energies, are shown in the Fig. 7. It may be noted that the observed imaginary parts of the DPP (W_{dpp}) have larger values in comparison to the real parts of the DPP (V_{dpp}) for the bare potentials

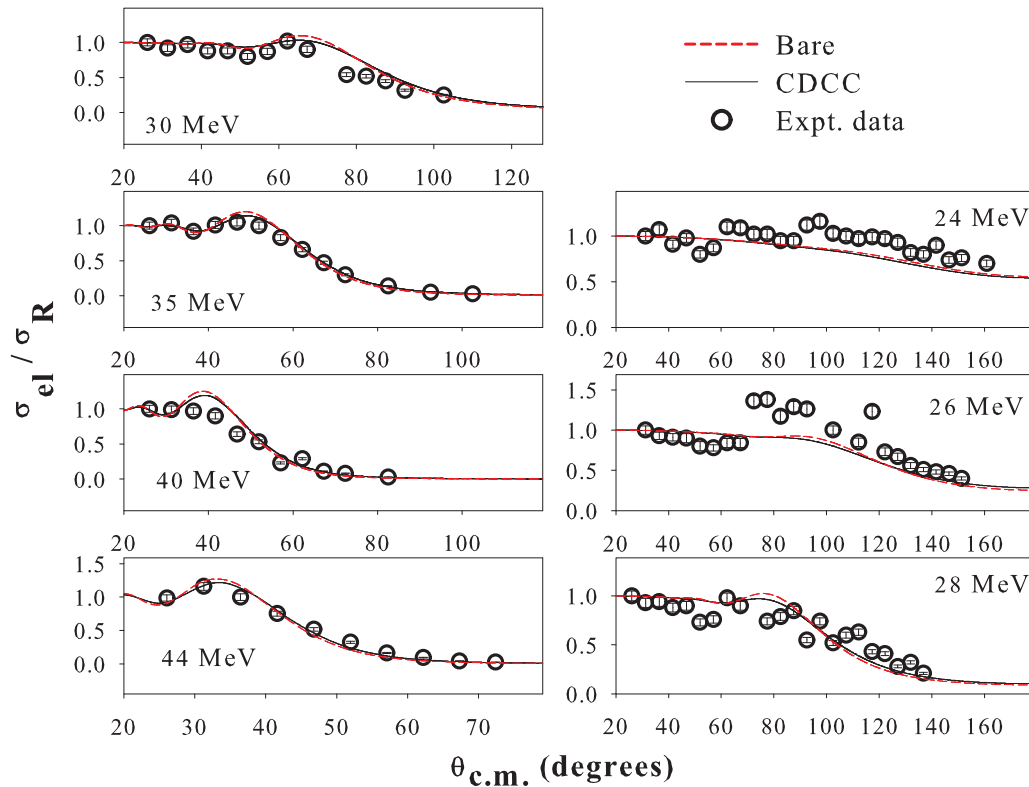


FIG. 5. (Color online) Experimental elastic-scattering cross sections normalized to the Rutherford cross sections as a function of $\theta_{c.m.}$ for the ${}^7\text{Li} + {}^{159}\text{Tb}$ system. The results of the CDCC calculation with and without including breakup couplings are shown by continuous and dashed lines, respectively.

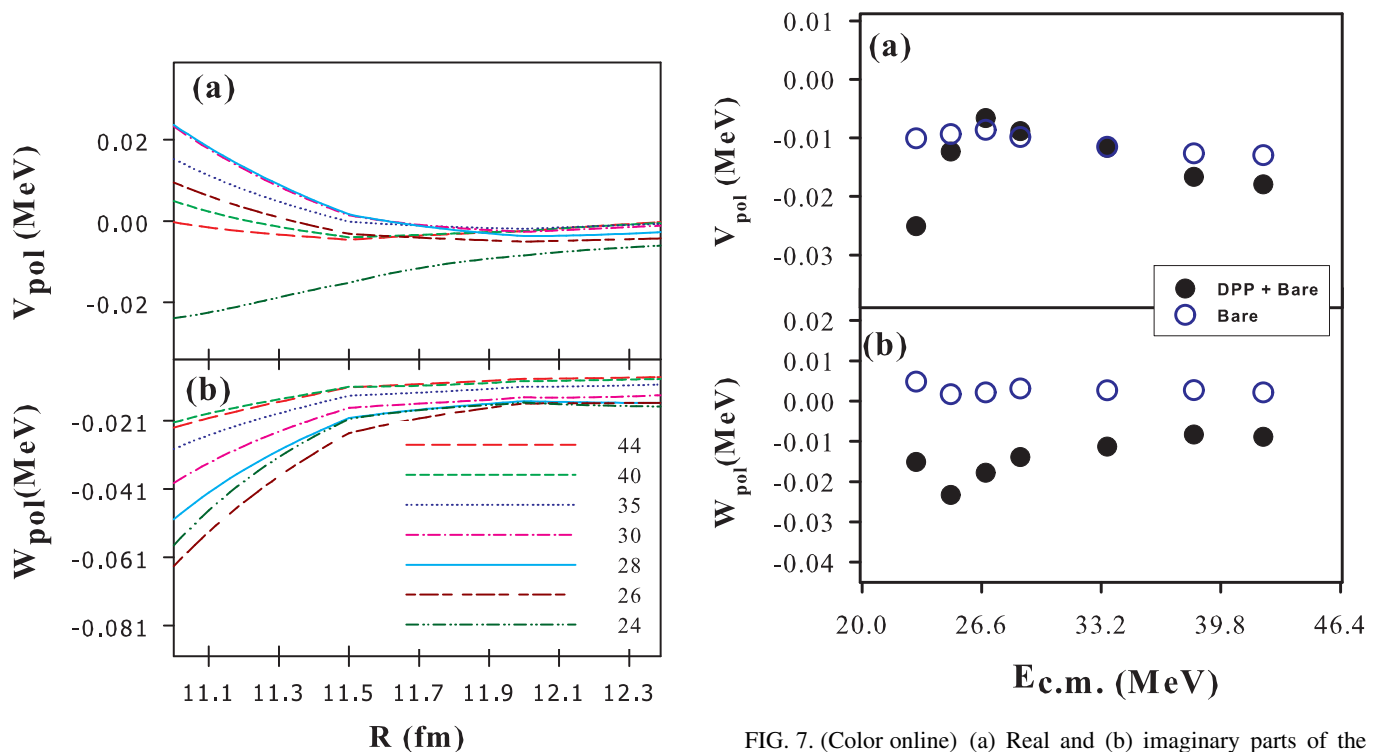


FIG. 6. (Color online) (a) Real and (b) imaginary parts of the dynamic polarization potentials (DPP) extracted from the CDCC calculation for the ${}^7\text{Li} + {}^{159}\text{Tb}$ system as a function of radius R .

FIG. 7. (Color online) (a) Real and (b) imaginary parts of the potential at an average radius $R_s = 11.5$ fm as a function of energy for the ${}^7\text{Li} + {}^{159}\text{Tb}$ system. The solid circles show dynamic polarization potentials (DPPs) extracted from the CDCC calculations and the open circles are the bare potentials which do not include any coupling.

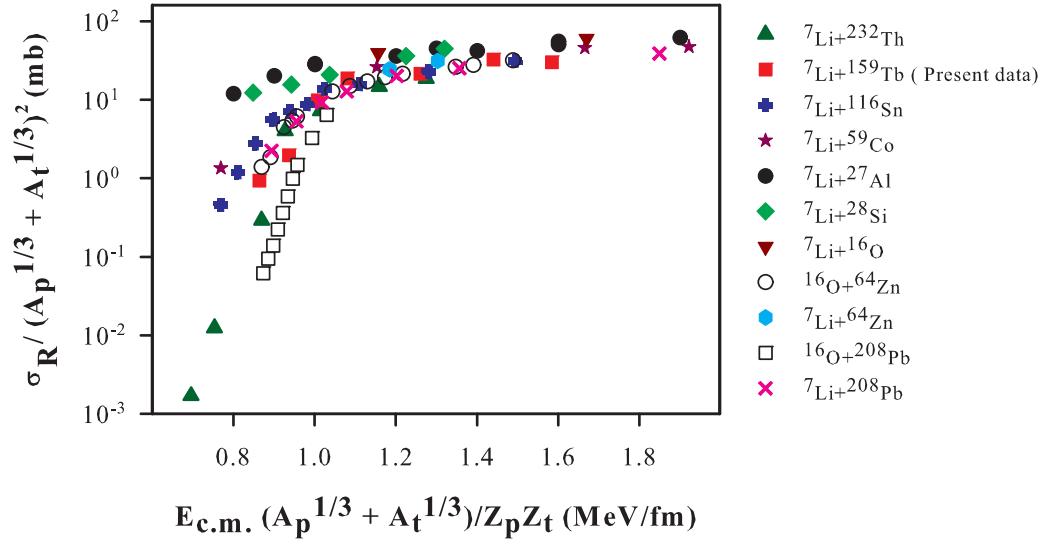


FIG. 8. (Color online) Comparison of reduced reaction cross sections for the reactions that involve ^7Li projectile and different target nuclei [4,12,15,16,23–28].

which do not include any coupling. The resultant attractive nature of nuclear potential could indicate the presence of the threshold anomaly. However, at below the barrier energies the imaginary part of the DPP (W_{dpp}) shows a sudden increase in strength and thus becomes less attractive in nature. Also, the net polarization potential, composed of competing attractive and repulsive parts, depends strongly on the bound state of the ^7Li projectile, target inelastic, transfer, and breakup channels.

V. TOTAL REACTION CROSS SECTIONS

A systematic study of total reaction cross sections involving ^7Li on various targets was carried out in the mass range $A = 16$ to 232. In order to perform a comparative study of excitation functions for different systems, it is required to suppress differences arising from the size and the charges of the systems. A reduction methodology proposed by Gomes *et al.* has been widely used for this kind of study [35]. In this method, the quantities $\sigma_R / (A_p^{1/3} + A_t^{1/3})^2$ vs $E_{c.m.} (A_p^{1/3} + A_t^{1/3}) / (Z_p Z_t)$ are plotted, where p and t are related to the projectile and target, respectively, and σ_R is the total reaction cross section. It was suggested that this procedure removes the dependence on the charge and mass of the collision partners but not on specific features of the projectile density, particularly when weakly bound projectile nuclei are involved. The total reaction cross sections in the case of ^7Li projectile and different target nuclei in the mass range $A = 16$ to 232 are shown in Fig. 8. Two sets of data for ^{16}O -induced reactions are also shown in Fig. 8. It is observed that the total reaction cross sections have target mass dependence at lower energies.

VI. SUMMARY AND CONCLUSIONS

Elastic-scattering angular distributions were measured at near barrier energies for the $^7\text{Li} + ^{159}\text{Tb}$ system. The optical-model analysis using the WSP potential, was carried

out to investigate the energy dependence of the interaction potential. The obtained behavior of the potential parameters show unusual energy dependence for their real and imaginary parts. It was seen that, as the bombarding energy decreases, the imaginary potential first increases at near barrier energy and then decreases as energy decreases. No strong conclusion could be made for the presence of the threshold anomaly which was confirmed earlier for the tightly bound systems.

Moreover, to investigate the effect of breakup coupling on the elastic channel, continuum-discretized coupled-channels (CDCC) calculations with the inclusion of the bound excited state of ^7Li and the target inelastic state, were carried out. The effects of breakup coupling on elastic-scattering angular distributions are observed to be small. The dynamic polarization potentials from the present CDCC calculations are studied with respect to the radius R as well as bombarding energies. The imaginary part of the polarization potential becomes more attractive as the energy decreases; however, at the lowest incident energy it shows a less attractive nature. The net effect of real and imaginary polarization potentials are observed to be attractive in nature, which reduces the barrier and may be responsible for the enhancement in the fusion cross sections. However, neither from the optical-model analysis nor from CDCC calculations could the presence of the threshold anomaly be confirmed.

A comparative study of total reaction cross sections for ^7Li projectile on different target nuclei in the mass range $A = 16$ to 232 shows that, at the lower-energy region, the total reaction cross section reduces as target mass increases.

ACKNOWLEDGMENTS

The authors thank the operating staff of the BARC-TIFR Pelletron facility (India) for the excellent operation of the machine during the experiment. One of the authors (D.P.) acknowledges financial support from Council of Scientific & Industrial Research, Govt. of India (Ack. No. 162033/2K12/1).

- [1] L. F. Canto, P. R. S. Gomes, R. Donangelo, and M. S. Hussein, *Phys. Rep.* **424**, 1 (2006).
- [2] B. B. Back, H. Esbensen, C. L. Jiang, and K. E. Rehm, *Rev. Mod. Phys.* **86**, 317 (2014).
- [3] G. R. Satchler, *Phys. Rep.* **199**, 147 (1991).
- [4] D. Patel, S. Santra, S. Mukherjee, B. K. Nayak, P. K. Rath, V. V. Parkar, and R. K. Choudhury, *Pramana J. Phys.* **81**, 587 (2013).
- [5] J. M. Figueira, D. Abriola, J. O. Fernandez Niello, A. Arazi, O. A. Capurro, E. de Barbara, G. V. Marti, D. Martinez Heimann, A. J. Pacheco, J. E. Testoni, I. Padron, P. R. S. Gomes, and J. Lubian, *Phys. Rev. C* **73**, 054603 (2006).
- [6] J. M. Figueira, J. O. Fernandez Niello, D. Abriola, A. Arazi, O. A. Capurro, E. de Barbara, G. V. Marti, D. Martinez Heimann, A. E. Negri, A. J. Pacheco, I. Padron, P. R. S. Gomes, J. Lubian, T. Correa, and B. Paes, *Phys. Rev. C* **75**, 017602 (2007).
- [7] A. Pakou, N. Alamanos, A. Lagoyannis, A. Gillibert, E. C. Pollacco, P. A. Assimakopoulos, G. Doukelis, K. G. Ioannides, D. Karadimos, D. Karamanis, M. Kokkoris, E. Kossionides, N. G. Nicolis, C. Papachristodoulou, N. Patronis, G. Perdikakis, and D. Pierroutsakou, *Phys. Lett. B* **556**, 21 (2003).
- [8] A. Pakou, *Phys. Rev. C* **78**, 067601 (2008).
- [9] F. A. Souza, L. A. S. Leal, N. Carlin, M. G. Munhoz, R. Liguori Neto, M. M. de Moura, A. A. P. Suaide, E. M. Szanto, A. Szanto de Toledo, and J. Takahashi, *Phys. Rev. C* **75**, 044601 (2007).
- [10] L. Fimiani, J. M. Figueira, G. V. Marti, J. E. Testoni, A. J. Pacheco, W. H. Z. Cardenas, A. Arazi, O. A. Capurro, M. A. Cardona, P. Carnelli, E. de Barbara, D. Hojman, D. Martinez Heimann, and A. E. Negri, *Phys. Rev. C* **86**, 044607 (2012).
- [11] N. N. Deshmukh, S. Mukherjee, D. Patel, N. L. Singh, P. K. Rath, B. K. Nayak, D. C. Biswas, S. Santra, E. T. Mirgule, L. S. Danu, Y. K. Gupta, A. Saxena, R. K. Choudhury, R. Kumar, J. Lubian, C. C. Lopes, E. N. Cardozo, and P. R. S. Gomes, *Phys. Rev. C* **83**, 024607 (2011).
- [12] N. N. Deshmukh, S. Mukherjee, B. K. Nayak, D. C. Biswas, S. Santra, E. T. Mirgule, S. Appannababu, D. Patel, A. Saxena, R. K. Choudhury, J. Lubian, and P. R. S. Gomes, *Eur. Phys. J. A* **45**, 23 (2010).
- [13] A. M. M. Maciel, P. R. S. Gomes, J. Lubian, R. M. Anjos, R. Cabezas, G. M. Santos, C. Muri, S. B. Moraes, R. L. Neto, N. Added, N. C. Filho, and C. Tenreiro, *Phys. Rev. C* **59**, 2103 (1999).
- [14] J. M. Figueira, J. O. Fernandez Niello, A. Arazi, O. A. Capurro, P. Carnelli, L. Fimiani, G. V. Marti, D. Martinez Heimann, A. E. Negri, A. J. Pacheco, J. Lubian, D. S. Monteiro, and P. R. S. Gomes, *Phys. Rev. C* **81**, 024613 (2010).
- [15] N. Keeley, S. J. Bennett, N. M. Clarke, B. R. Fulton, G. Tungate, P. V. Drumm, M. A. Nagarajan, and J. S. Lilley, *Nucl. Phys. A* **571**, 326 (1994).
- [16] S. Dubey, S. Mukherjee, D. C. Biswas, B. K. Nayak, D. Patel, G. K. Prajapati, Y. K. Gupta, B. N. Joshi, L. S. Danu, S. Mukhopadhyay, B. V. John, V. V. Desai, S. V. Suryanarayana, R. P. Vind, N. N. Deshmukh, S. Appannababu, and P. M. Prajapati, *Phys. Rev. C* **89**, 014610 (2014).
- [17] K. Zerva, A. Pakou, N. Patronis, P. Figuera, A. Musumarra, A. Di Pietro, M. Fisichella, T. Glodariu, M. La Commara, M. Lattuada, M. Mazzocco, M. G. Pellegriti, D. Pierroutsakou, A. M. Sanchez-Benitez, V. Scuderi, E. Strano, and K. Rusek, *Eur. Phys. J. A* **48**, 102 (2012).
- [18] K. Zerva, A. Pakou, K. Rusek, N. Patronis, N. Alamanos, X. Aslanoglou, D. Filipescu, T. Glodariu, N. Keeley, M. Kokkoris, M. La Commara, A. Lagoyannis, M. Mazzocco, N. G. Nicolis, D. Pierroutsakou, and M. Romoli, *Phys. Rev. C* **82**, 044607 (2010).
- [19] J. Raynal, *Phys. Rev. C* **23**, 2571 (1981).
- [20] D. Abriola *et al.*, *Phys. Rev. C* **39**, 546 (1989).
- [21] D. Abriola *et al.*, *Phys. Rev. C* **46**, 244 (1992).
- [22] C. Mahaux, H. Ngo, and G. R. Satchler, *Nucl. Phys. A* **449**, 354 (1986).
- [23] K. Kalita, S. Verma, R. Singh, J. J. Das, A. Jhingan, N. Madhavan, S. Nath, T. Varughese, P. Sugathan, V. V. Parkar, K. Mahata, K. Ramachandran, A. Shrivastava, A. Chatterjee, S. Kailas, S. Barua, P. Basu, H. Majumdar, M. Sinha, R. Bhattacharya, and A. K. Sinha, *Phys. Rev. C* **73**, 024609 (2006).
- [24] C. Beck, N. Keeley, and A. Diaz-Torres, *Phys. Rev. C* **75**, 054605 (2007).
- [25] P. R. S. Gomes *et al.*, *Phys. Rev. C* **71**, 034608 (2005).
- [26] N. Keeley, K. W. Kemper, and K. Rusek, *Phys. Rev. C* **65**, 014601 (2001).
- [27] A. Pakou *et al.*, *Nucl. Phys. A* **784**, 13 (2007).
- [28] V. V. Sargsyan, G. G. Adamian, N. V. Antonenko, and P. R. S. Gomes, *Phys. Rev. C* **88**, 044606 (2013).
- [29] I. J. Thompson, *Comput. Phys. Rep.* **7**, 167 (1988).
- [30] A. Diaz-Torres, I. J. Thompson, and C. Beck, *Phys. Rev. C* **68**, 044607 (2003).
- [31] N. Keeley, R. Raabe, N. Alamanos, and J. L. Sida, *Prog. Part. Nucl. Phys.* **59**, 579 (2007).
- [32] N. Keeley, N. Alamanos, K. W. Kemper, and K. Rusek, *Prog. Part. Nucl. Phys.* **63**, 396 (2009).
- [33] D. Patel, S. Mukherjee, B. K. Nayak, S. V. Suryanarayana, D. C. Biswas, E. T. Mirgule, Y. K. Gupta, L. S. Danu, B. V. John, and A. Saxena, *Phys. Rev. C* **89**, 064614 (2014).
- [34] C. Vargas, J. G. Hirsch, T. Beuschel, and J. P. Draayer, *Phys. Rev. C* **61**, 031301 (2000).
- [35] P. R. S. Gomes, J. Lubian, I. Padron, and R. M. Anjos, *Phys. Rev. C* **71**, 017601 (2005).